Phase and orientational ordering of low molecular weight rod molecules in a quenched liquid crystalline polymer matrix with mobile side chains

Lorin Gutman, Jianshu Cao,[a] and Tim M. Swager
Department of Chemistry, Massachusetts Institute of Technology, Cambridge, Massachusetts 02139-4307

We study the phase diagram and orientational ordering of guest liquid crystalline (LC) rods immersed in a quenched host made of a liquid crystalline polymer (LCP) matrix with mobile side chains. The LCP matrix lies below the glass transition of the polymer backbone. The side chains are mobile and can align to the guest rod molecules in a plane normal to the local LCP chain contour. A field theoretic formulation for this system is proposed and the effects of the LCP matrix on LC ordering are determined numerically. We obtain simple analytical equations for the nematic/isotropic phase diagram boundaries. Our calculation show a nematic–nematic (N/N) first order transition from a guest stabilized to a guest–host stabilized region and the possibility of a reentrant transition from a guest stabilized nematic region to a host only stabilized regime separated by an isotropic phase. A detailed study of thermodynamic variables and interactions on orientational ordering and phases is carried out and the relevance of our predictions to experiments and computer simulations is presented. © *2004 American Institute of Physics.* [DOI: 10.1063/1.1739211]

I. INTRODUCTION

Liquid crystal (LC) technology is relevant to many applications that include spatial light modulators, high strength fibers, chromatographic separations, and liquid crystals displays to name a few. In these applications the LC orientational performance is strongly effected by the conformational organization and anisotropy of the host matrix and the molecular interaction among the host and the low molecular weight guest. Control and manipulation of properties and ordering in the glassy matrix, the LC morphology inside the matrix and the nature of interactions ordering of the short LC molecular rods is crucial for practical applications.[1]

Below we review theoretical and experimental progress made in understanding and manipulating material and phase properties in relevant liquid crystalline systems. Liquid crystal rods have been studied in the framework of Landau–de Gennes expansion.[2] In principle, the truncation of the perturbation expansion at a finite order is questionable for a first order $N–I$ transition, but the framework is convenient and efforts were made to adapt it to short rods and LC polymers. Inclusion of the density dependence in the orientational Landau expansion[3] allows a closer proximity among theoretical predictions for the $N–I$ transition/thermodynamic quantities and experiments.

Another instrumental framework to model orientational ordering in experiments of short LC rods is the Mayer–Saupe self-consistent theory.[4] This approach is free of free energy truncations and widely used in experimental analysis of thermotropic LC.[5] Recently, the Mayer–Saupe approach has also been extended to study lyotropic ordering in PAA measured in SANS and nuclear magnetic resonance (NMR) experiments.[6] Predictions from the modified Mayer–Saupe theory for the $N–I$ density threshold were found in good agreement with the experimental results yet the ordering in the nematic phase was slightly underestimated.

Dynamical regimes in liquid crystals in the isotropic phase were explored to a limited extent.[7] Studies in LC of 3CHBT in the 1 ps–100 ns time domain showed in the long time limit an exponential relaxation of the orientational scattering function in agreement with prediction from a dynamical Landau theory. The orientational function diverges at the N/I transition and the Kerr effect measurements show a power law decay at short times. The power law was ascribed to intradomain dynamics and the exponential Landau–de Gennes decay was attributed to decay of orientational relaxation of pseudodomains. Two scaling temperatures were[8] observed at lower temperatures and attributed to two typical relaxation processes: one from the caging effect also present in isotropic liquids and the other from the freezing of orientations. These signatures suggest the possibility of "two glass transitions" in nematic LCs. Using a continuum approach, strain effects on thermal stability of a rod matrix to a radial perturbation and bounds for rod instability were elucidated.[9]

In many situations of practical interest low molecular LC rods are found in some sort of quenched external disorder. The effect of an environment that carries a quenched isotropic disorder was investigated by computer simulations and also experiments. Monte Carlo studies[10] showed that 5% quenched impurities can make the $N–I$ transition weakly first order and even suppress it. These predictions have support from NMR measurements[11] on 8CB LCs confined to a silica aerogel. Decrease in pore size flattens the $N–I$ transi-

---
[a]Author to whom correspondence should be addressed. Electronic mail: jianshu@mit.edu

tion and modifies the transition order below a critical aerogel density.

The matrix surrounding the rod molecules is often constructed from polymers instead of aerogels, when optimal optical properties in LC display applications and light control devices as optical shutters are of interest. In this regard simple theories of a mixture of flexible polymers and short rods have been proposed. The theory combines the Flory–Huggins approach for the translational entropy and isotropic segment interactions of the polymer with the Mayer–Saupe method[12] to describe interaction and orientational anisotropy. The theory predictions, i.e., liquid–liquid, isotropic–nematic, and isotropic–smectic transitions have some support from differential scanning calorimetry and optical microscopy experiments on 8CB and linear polystyrene.[13]

Polymer matrix dispersed with LC droplets (PDLCs) were studied in dynamic light experiments.[14] In these systems the effects of the matrix cavities on the LC droplets are of interest. In the absence of an external field the orientational diffusivity observed was below the bulk ordering and the magnitude of the average scattering vector was of the order of the droplet diameter. In the presence of an electric field an increase in inverse relaxation time with increasing temperature near the $N-I$ transition was observed. A more comprehensive analysis of external field effects in PDLC were studied by Monte Carlo simulations for different droplet boundary conditions.[15] Predictions for NMR spectra that correspond to different simulation scenarios were also computed. In C^{13} NMR, and polarized optical microscopy experiments the polymer matrix was partially ordered due to interdigitation of the 5CB ordered LC molecules in the droplets.[16]

One way to manipulate optical properties in guest–host systems is using dipolar guest chromophores. The dipole displacement from the chromophore center of mass can be quenched by immersion of the chromophore in a liquid polymer matrix subject to a strong poling field (viz. see Ref. 17 for details). This process of setting the macroscopic asymmetry is instrumental for construction of materials with macroscopic nonlinear optical properties that manifest in the presence of much weaker fields. Simple models for this system have been proposed[18] and predictions were found in reasonable agreement with experiments.[19–21]

Another way to optimize electro–optical properties is by adding mesogen side chain to the polymer matrix. Experiments on C5 and C3 liquid crystal polymer (LCP)[22] probed the nematic ordering in side chain polymer liquid crystals.[22] The measured $N-I$ transition was weakly first order in the absence of a magnetic field, but becomes a strong first order transition. This effect of an external field was attributed to the suppression of the nematic order fluctuations due to alignment with the field director. Few mechanisms for grafting side chains to the polymer matrix were investigated. In one case the polymer matrix carries low molar mass receptors for the side chain mesogens. This mechanism for amplification of liquid crystallinity is of great relevance for molecular electronics applications.[23]

A related experimental study explored the use of hydrogen bonded host–guest system. The LCP with side chains host was made of acrylate and 4-vinyl-pyridine copolymer
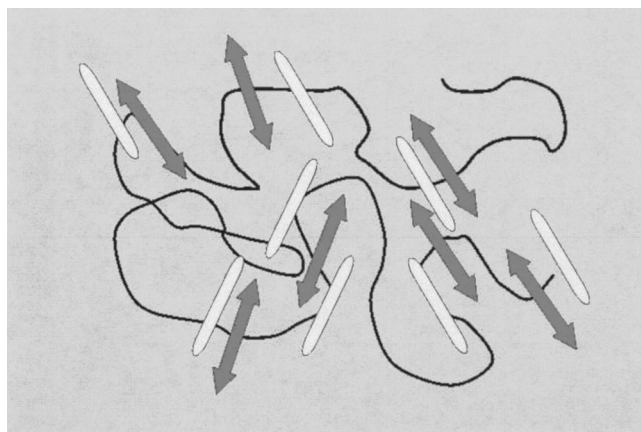

FIG. 1. LC rods (elongated ellipsoids) in a LCP quenched matrix (thick solid line) with mobile side chains (double headed arrows).

and the low molecular weight LC was guest aso-benzene. Ultraviolet (UV) and visible light irradiation experiments showed the occurrence of reversible photochemical $N-I$ and $I-N$ transitions due trans–cis/cis–trans guest isomerization.[24] The use of a host made of a LCP with side chains facilitated improved wide angle view ability and a better optical transmittance in the ON state of the applied electric field. This finding suggests that the presence of side chains in a LCP host may offer better opportunities to manipulate electro–optical properties than a LCP host.

Experiments show that the refractive index of the side chains can be matched with the refractive index of the low molecular weight LC. A simple theory of LCP/LC guest–host system that combines the Flory–Huggins approach and the Mayer–Saupe like contributions to LCP side chains and LC low molecular rods anisotropy was proposed. The theory was used to study phase ordering in an epoxy resin with mesogenic amines and a low molecular weight LC (E7) guest.[25] The coupling of side chain orientations to polymer conformations was neglected in this work. That theory aims to describe equilibrium miscible/imiscible mixtures of LCP polymer and LC rods. In the imiscible case it predicts an isotropic phase $N-I$ and a single nematic phase.[26]

In the present work we develop a rigorous field theory of a more complex guest–host system. The host is a stiff LCP homopolymer matrix quenched below the glass transition of the backbone. The side chains are mobile and can rotate freely in the plane normal to the LCP local chain contour. In the homopolymer matrix there are also free low molecular rod shaped molecules that are not attached to the matrix. The interaction alignment of the polymer backbone segments is assumed to be strong and the guest–host interactions do not affect the host backbone alignment. The host backbone conformations provide an anisotropic quenched disordered glassy like media for the low molecular weight rods. While the LCP backbone is quenched the side chains on the LCP can rotate freely in the plane perpendicular to the backbone LCP contour and equilibrate with the guest. The physical scenario just described is depicted in Fig. 1. Some aspects of the equilibrated LCP/LC mixture have been studied;[25,26] the

scenario proposed here opens new avenues for manipulating orientational ordering in materials.

One important feature suggested in recent experiments is the manipulation of the free volume in the host matrix. Optical materials that display guest–host microscopic orientational ordering were synthesized recently.[27] Optimization of free volume for alignment was used in these experiments to increase guest–host ordering and LC alignment, decrease switching response times, and overall for a better material performance in holographic data storage applications. Orientation can also couple to electronic structure;[28] triptycene molecules were found instrumental to redirect and enhance molecular alignment due to a natural tendency of the guest–host system to lower free energy by free volume minimization.

Triptycene bound polymers can display mesomorphic behavior in a glassy state in the absence of distinct crystallization. Glassy mesophases using triptycenes[29] in single component LCs have a relatively slow response times. In principle biaxial ordering can allow faster switching times from flips normal to the backbone molecular director of the polymer host, yet biaxial ordering in most cases is not stable in homopolymers. Another approach that promotes fast switching times and also guides guest ordering uses side chains mobile in the plane normal to the matrix director.

In the present work we explore numerically the orientational phase ordering of LC rod molecules in a host glassy polymer with mobile side chains using a theoretical framework that does not invoke the Landau expansion employed in other systems.[30] The present approach is suitable to analyze experiments further away from critical points.

II. THEORY DEVELOPMENT

The microscopic Hamiltonian for the guest–host LC/ LCP system is

$$H=\sum_{i=1}^{N}\int_0^L \frac{\beta\epsilon}{2}\dot{\mathbf{u}}^2(n_i)dn_i-\frac{w_{r,r}}{2}\sum_{k,l=1}^{M,M}\delta(\mathbf{r}_k-\mathbf{r}_l)(1-(\mathbf{u}_k\times\mathbf{u}_l)^2)-w_{r,p}\sum_{i,k=1}^{N,M}\int_0^L dn_i\delta(\mathbf{r}(n_i)-\mathbf{r}_k)(1-(\mathbf{u}(n_i)\times\mathbf{u}_k)^2)$$

$$-\frac{w_{p,p}}{2}\sum_{i,j=1}^{N,N}\int_0^L dn_i\int_0^L dn_j'\,\delta(\mathbf{r}(n_i)-\mathbf{r}(n_j'))(1-(\mathbf{u}(n_i)\times\mathbf{u}(n_j'))^2),\tag{1}$$

where i and j are chain indexes, k and l are indexes for the short molecular rods, M is the number of short rods, and N is the number of polymer chains. $\mathbf{r}(n_i)$ is the spatial location of the nth segment on the ith chain, $\mathbf{u}(n_i)$ is the tangent vector at n_i on the backbone of the ith polymer chain, $\mathbf{r}_k$ is the spatial location of the kth rod, and $\mathbf{u}_k$ is the director of the kth rod.

Let us now explain the Hamiltonian in Eq. (1). The first term in Eq. (1) is the interaction potential among adjacent segments in semiflexible noninteracting LCP chains, and $\beta\epsilon/2$ is the local penalty from bending the polymer chain. The second, third, and fourth term in Eq. (1) represent the rod–rod, rod–polymer segment, and polymer segment– polymer segment microscopic anisotropic interactions, respectively. The short range anisotropic potential among molecular species has the form:

$$\frac{w_{o,m}}{2}\sum_{o,m}\delta(\mathbf{r_o}-\mathbf{r}_m)(1-(\mathbf{u_o}\times\mathbf{u}_m)^2).$$

Positive values of w promote director alignment of the molecules o and m. Negative w values favor configurations where the director of the mth molecule is perpendicular to that of the oth molecule. For the guest–host system $w_{p,p}$ and $w_{r,r}$ are positive and favor alignment of polymer–polymer backbone segments and rod–rod directors, respectively. $w_{r,p}$ is chosen to have a negative value and stabilizes alignment of the short molecular rods in a plane perpendicular to the

chain backbone from interaction of the short rods with backbone side chains.

Most generally,[31] the short range anisotropic interaction potential w contains athermal and soft interaction contributions[31]

$$w=v+V(T)/kT.\tag{2}$$

Interaction-wise, our model describes adequately the inter/ intra microscopic anisotropy of the LC and LCP mixed system and it includes athermal repulsive contributions and a soft temperature dependent attraction term. The usage of short range interactions in the Hamiltonian (viz. Ref. 32 for a review of basic LC models) also employed in the study of other liquid crystalline systems[33,34] is adequate only when the physical phenomena studied extend over spatial scales that are large compared with the interaction range present in the guest–host system.

Let us now outline the solution steps that lead to computation of the free energy for the guest–host system. First, we express Eq. (1) with orientational tensors

$$H=\sum_i\int\frac{\beta\epsilon}{2}\dot{\mathbf{u}}^2(n_i)dn_i$$

$$+\sum_{m,o=p,r}\left(w_{m,o}\int d\mathbf{r}[\hat{\sigma}_m^{ii}(\mathbf{r})\hat{\sigma}_o^{jj}(\mathbf{r})-\hat{\sigma}_m^{ij}(\mathbf{r})\hat{\sigma}_o^{ji}(\mathbf{r})]\right.$$

$$\left.+u_{m,n}\int d\mathbf{r}\hat{\rho}_m(\mathbf{r})\hat{\rho}_o(\mathbf{r})\right).\tag{3}$$

The index values of m and o, i.e., r and p, stand for LC rods and LCP segments, respectively. The microscopic densities — $\rho_m(\mathbf{r})$ and orientational tensors — $\sigma_m(\mathbf{r})$ are given by

$$\hat{\rho}_p(\mathbf{r}) = \sum_i \int dn_i \delta(\mathbf{r} - \mathbf{r}(n_i));$$

$$\rho_r = \sum_k \delta(\mathbf{r} - \mathbf{r}_k);$$

$$\hat{\sigma}_p^{st}(\mathbf{r}) = \sum_i \int dn_i \delta(\mathbf{r} - \mathbf{r}(n_i)) \mathbf{u}_p^s(n_i) \mathbf{u}_p^t(n_i) i$$

$$= \sum_k \delta(\mathbf{r} - \mathbf{r}) \mathbf{u}_{r,k}^s \mathbf{u}_{r,k}^t, \tag{4}$$

where the indexes s, t stand for the x, y, z space component indexes. Usage of orientational tensors in calculation of the free energy (viz. see also Ref. 31) retains the relation among orientational ordering of different molecular species in the Hamiltonian and the manifestation of this relation in the physics displayed by the guest–host phase diagrams and orientational ordering profile.

Now, we impose delta function constraints on the partition function of the guest–host system and exchange discrete with continuous microscopic orientational tensors for LC rods and LCP segments. A global constraint set on chain director fluctuations of the LCP segments is sufficient due to chain connectivity (viz. see Ref. 31 for further details). The LC rod endpoints are free and a local constraint is required on rod orientational fluctuations. The partition function for the guest–host system is given by

$$Z[\mathbf{u}(n_i), \mathbf{u}_k] = \iint \left[\prod_{n_i, \mathbf{r}} \int d\mathbf{r}^k \int d\mathbf{u}^k D\mathbf{r}_i(n_i) \right.$$

$$\times \left. \prod_{m=p,r,\mathbf{r}} D\sigma_m(\mathbf{r}) \right] \exp(-H[\sigma_m(\mathbf{r})])$$

$$\times \prod_{n_i,\mathbf{r}} \delta[\sigma_p(\mathbf{r}) - \hat{\sigma}_p(\mathbf{r})] \delta[\mathbf{u}(n_i)^2 - 1]$$

$$\times \prod_{k,\mathbf{r}} \delta[\sigma_r(\mathbf{r}) - \hat{\sigma}_r(\mathbf{r})] \delta[\mathbf{u}_k^2 - 1], \tag{5}$$

$\hat{\sigma}_m(\mathbf{r})$ are given in Eq. (1); the $\hat{\sigma}_m(\mathbf{r})$ delta function constraints are expressed with auxiliary fields $\psi_m(\mathbf{r})$. The disorder here represented by the matrix conformations is external to the fluid of interest and replicas are not needed for disorder averages

$$Z[\mathbf{u}(n_i), \mathbf{u}_k] = \iint \left[\prod_{n_i, \mathbf{r}} \int d\mathbf{r}^k \int d\mathbf{u}^k D\mathbf{r}_i(n_i) \prod_{m=p,r,\mathbf{r}} \int D\psi_m(\mathbf{r}) D\sigma_m(\mathbf{r}) \right] \exp(-H[\hat{\sigma}_m(\mathbf{r})])$$

$$\times \prod_{n_i,\mathbf{r}} \exp\left(i \int d\mathbf{r} \psi_p(\mathbf{r}) : [\sigma_p(\mathbf{r}) - \hat{\sigma}_p(\mathbf{r})] \right) \int d\lambda_p \exp(-i\lambda_p[\mathbf{u}(n_i)^2 - 1])$$

$$\times \prod_{k,\mathbf{r}} \int d\lambda_{r,k} \exp\left(i \int d\mathbf{r} \, \psi_r(\mathbf{r}) : [\sigma_r(\mathbf{r}) - \hat{\sigma}_r(\mathbf{r})] \right) \exp\left[-i \sum_k (\lambda_{r,k}(\mathbf{u}_k^2 - 1)) \right], \tag{6}$$

where k is the index of the rods. Most generally, the orientational tensor matrix for the molecular species — $m = r, p$, in principal axis representation has the form

$$\sigma_m = \begin{pmatrix} a_m - b_m & 0 & 0 \\ 0 & a_m - b_m & 0 \\ 0 & 0 & 2a_m \end{pmatrix}. \tag{7}$$

Our present work centers on the orientational phase diagram and the relation among uniaxial ordering of the guest and host described by the order parameter $\langle S \rangle_m$:

$$\langle S \rangle_m = 0.5 \frac{V}{N_m} \sum_\alpha \langle 3(\mathbf{v}_m^\alpha \cdot \mathbf{n}_m)^2 - 1 \rangle, \tag{8}$$

where $\mathbf{v}_m^\alpha$ is the unit vector that points along the long axis of molecule α of type m located at $\mathbf{r}^\alpha$ and N_m is the number of molecules of type m present in the system.

For uniaxial ordering, the orientational order parameter, $\langle S \rangle_m$ is related to the principal axis components of the orientational tensor in the following way: $\langle S \rangle_m = (-3a_m/b_m)$.

$1 > \langle S \rangle_m > 0$ signals uniaxial nematic ordering while $-0.5 < \langle S \rangle_m < 0$ signals discotic ordering. In Einstein notation (alike indexes are summed over), $\sigma_m^{i,i} = \rho_m$.

Let us now turn our attention to derivation of the guest–host system free energy. Contributions to free energy from LC rods are calculated in Appendix A and LCP contributions to free energy are obtained in Appendix B. These contributions do not involve the coupling between the guest and the host and are each calculated in a separate principal axis representation of σ_r and σ_p, respectively.

Calculation of the guest–host coupling term $\text{Tr}(\sigma_r : \sigma_p)$ is a bit more involved and is evaluated in Appendix C. Using Legendre transforms we obtain the free energy dependence on $\langle S \rangle_r$ and $\langle S \rangle_p$. In this calculation the LCP orientational fields are obtained via a self-consistent field (SCF) calculation that does not equilibrate the LCP fields to LC ordering. The LCP orientational ordering fields obtained act as external fields in the numerical calculation of orientational LC ordering that follows. Details of this calculation are discussed in Appendix D. The final free energy for the guest–host system, used in the numerical analysis of orientational phase ordering, is

$$F(\langle S\rangle_r,\lambda_p,\langle S\rangle_p)=\frac{w_{r,r}\rho_r^2}{3}(\langle S\rangle_r^2+\langle S\rangle_r+1)+\rho_r\log\left(\frac{\rho_r}{2\pi^2}\right)-0.572365\rho_r-\frac{2}{3}\rho_r\rho_p w_{p,r}+\left[\cos(\theta)^2-\frac{1}{3}\right]\langle S\rangle_p\rho_r\rho_p w_{p,r}$$

$$-\rho_r\log\left[\frac{\mathrm{erfi}[\sqrt{-w_{p,r}\rho_p\langle S\rangle_p+w_{r,r}\rho_r\langle S\rangle_r+3\rho_p w_{p,r}\langle S\rangle_p\cos(\theta)^2}]}{\sqrt{-w_{p,r}\rho_p\langle S\rangle_p+w_{r,r}\rho_r\langle S\rangle_r+3\rho_p w_{p,r}\langle S\rangle_p\cos(\theta)^2}}\right]+\rho_p\left[-\lambda_p+w_{p,p}\frac{1}{3}\rho_p(1+\langle S\rangle_p)\right.$$

$$\left.\times(1-\langle S\rangle_p)+\frac{2}{\beta\epsilon}\left[\left(\lambda_p+\rho_p\left(\frac{2}{3}(1-\langle S\rangle_p)w_{p,p}\right)\right)^{1/2}+2\left(\lambda_p+\rho_p\frac{2}{3}\left(1+\frac{\langle S\rangle_p}{2}\right)w_{p,p}\right)^{1/2}\right]\right]. \tag{9}$$

erfi in Eq. (9) is the imaginary error function.[36] The first terms are energetic contributions from LC rod–rod anisotropic interactions; the second term is the LC rod translational entropy. The next three terms are contributions from LC/LCP energetic anisotropic coupling. The sixth term has contributions to LC orientational entropy from the LC orientations coupled to polymer conformations and orientations of the LCP side chains. θ (viz. Appendix C) is the angle among the vectors perpendicular to the polymer matrix nematic ordering and the director of the rod ordering. $\theta=\pi/2$ and a negative $\langle S\rangle_r$ indicates discotic ordering in the plane normal to the polymer matrix nematic director, while $\theta=0$ and a positive $\langle S\rangle_r$ show the presence of nematic ordering in the plane perpendicular to the polymer matrix nematic director. The seventh term is the energetic contribution from anisotropic self-interactions of the LCP segments. The last term in the free energy is the entropic contribution from coupled orientations and conformations of the LCP matrix at fixed center of mass.

The limit $\rho_r\to0$ of Eq. (9) recovers the free energy of a many-chains LCPs solution without the Flory–Huggins translational entropy also obtained in Eq. (32) of Ref. 31, and the minimal value for uniaxial ordering $\langle S\rangle_p=0.25$, is reproduced herein.

The $\rho_p\to0$ limit of Eq. (9) recovers the Mayer–Saupe result for the magnitude of the orientational ordering at the $N-I$ transition, i.e., $\langle S\rangle_r=0.42$. The anisotropic interaction threshold for orientational ordering at $\rho_r=1$ is 1.5 times the Mayer–Saupe threshold, 4.52. Our result $w_{r,r}=6.78$ is consistent with the infinitely stiff limit of long worm like chains obtained from a field theoretic approach[37] of $w\cong7$. The temperature dependent phase diagram line for the guest–host $N-N$ transition is obtained using Eq. (2):

$$\rho_{c1}=\frac{v_{p,p}\left(1+\frac{T_p^s}{T_p^c}\right)-\frac{5.92T_p^c}{\epsilon}}{v_{p,p}\left(1+\frac{T_p^s}{T_p^c}\right)},$$

where $T_p^s=V_{p,p}/v_{p,p}$ is a measure of the polymer–polymer anisotropic interaction softness and T_p^c is the softness temperature for the nematic/isotropic of the host. The guest stabilized $N-I$ phase diagram line is

$$\rho_{c2}=\frac{T_r^c6.814}{v_{r,r}\left(1+\frac{T_r^s}{T_r^c}\right)}.$$

$T_r^s=V_{r,r}/v_{r,r}$ is a measure of the short rod–rod anisotropic interaction softness and T_r^c is the temperature for the nematic/isotropic of the rods in the absence of the host.

The free energy of the guest–host system is minimized analytically with respect to the fields ($\langle S\rangle_p,\lambda_p$), first, in the absence of the LCP–LC rod interaction anisotropic coupling. The value of $\langle S\rangle_p$ and λ_p obtained from numerical solution of the SCF relations for $\langle S\rangle_p$ and λ_p, is used in $F(\langle S\rangle_r,\lambda_p,\langle S\rangle_p)$, and the free energy is now optimized in the presence of orientational ordering of the LCP matrix with respect to $\langle S\rangle_r$ at a measurement angle normal to the LCP director.

The unit length chosen in all calculations, the monomer hard sphere (temperature independent) diameter, renders chain microscopic interactions and characteristics, L, $\beta\epsilon$, w, v, and ρ dimensionless.

III. DISCUSSION OF RESULTS

Let us now discuss the predictions from the numerical analysis for orientational ordering profiles of LC rods in the presence of an LCP matrix in different phase regions.

Figure 2 is a numerical study of effects of LCP–LCP interaction anisotropy-$w_{p,p}$, LC–LCP interaction anisotropy rod–$w_{p,r}$, and LC rod density on orientational ordering of
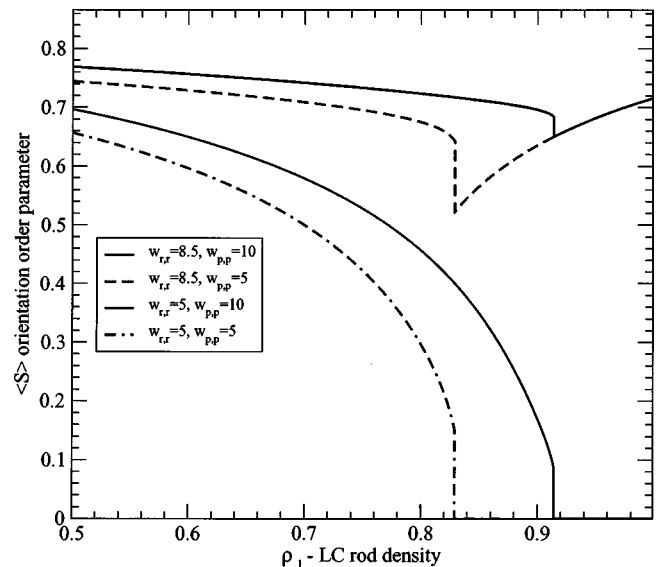
FIG. 2. Effect of variation of alignment interaction in LCP matrix on ordering in LC rods: guest–host anisotropic coupling, $w_{p,r}=5$, chain stiffness $\beta\epsilon=7$.
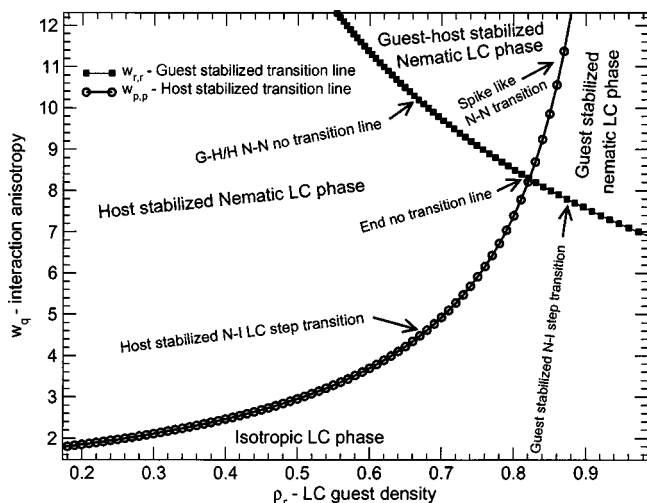
J. Chem. Phys., Vol. 120, No. 23, 15 June 2004

Phase and orientational ordering   11321

FIG. 3. Orientational phase diagram for LC rods in guest–host polymer matrix: $q = (p,p)$ and (p,r), $w_{p,r} = 4$, $\beta\epsilon = 5$.

the LC rods. Only stable solutions are plotted. The x axis, ρ_r, is also $1 - \rho_p = \rho_r$ where ρ_p is the backbone density of the quenched polymer matrix. At high guest densities, for $\rho_r > 0.92$ and $w_{r,r} = 8.5$ in Fig. 2, ordering is stabilized by guest anisotropy alone. Below that density, for $w_{r,r} = 8.5$ the LCP quenched matrix undergoes a $N-I$ phase transition. The N/I ordering of the matrix restricts the effective spatial dimension in which the LC rods can order to a sheet of finite width. The nematic matrix alignment stabilizes the discotic crowding of the rods in a plane perpendicular to the backbone LCP director. The magnitude of the nematic rod ordering in that plane given by $\langle S \rangle_r$, changes discontinuously via a first order $N-N$ transition. The form of the discontinuity in $\langle S \rangle_r$ in the vicinity of the $N-N$ transition resembles a spike rather than a step like transition. We loosely term it a spike like transition. For $w_{r,r} = 5.0$ and $\rho_r > 0.92$ in Fig. 2, the guest interaction alignment anisotropy is weak and guest stabilized ordering is precluded. At this value of $w_{r,r}$ the LCP matrix orders the guest for $\rho_r < 0.92$ via a first order step transition. In this case the orientational order parameter threshold $\langle S \rangle_r$ may be weaker then a typical Mayer–Saupe transition; the degree of ordering is determined by the guest–host coupling strength, $w_{p,r}$. This issue illustrated in Fig. 8 will be discussed later. The occurrence of a host stabilized nematic region suggests new ways to induce orientational ordering of guest LC rods and manipulate optical properties in applications.

Figure 3 is a concise and useful representation of the three-dimensional (3D) guest–host phase diagram. The y axis is w_q with $q = (p,p)$ and (r, r) (viz. the legend). The phase diagram lines are $w_{r,r}^c(\rho_r)$ (filled squares) the guest stabilized phase transition line, and $w_{p,p}^c(\rho_r)$ (empty circles), the host stabilized phase transition line. A thermodynamic state is described here by a point $(w_{p,p}, w_{r,r}, \rho_r)$. The LCP stiffness in Fig. 3 is fixed at $\beta\epsilon = 7$. For $w_{p,p} < w_{p,p}^c(\rho_r)$ and $w_{r,r} < w_{r,r}^c(\rho_r)$, the guest is found in the isotropic state. For $w_{p,p} < w_{p,p}^c(\rho_r)$, as $w_{r,r}$ crosses over above the $w_{r,r} = w_{r,r}^c(\rho_r)$ line, a guest stabilized nematic state forms via a first order Mayer–Saupe first order transition. For $w_{r,r}$

$< w_{r,r}^c(\rho_r)$ and $w_{p,p}$ crosses over above the $w_{p,p} = w_{p,p}^c(\rho_r)$ phase boundary the guest orders via a weak first order step transition to a host stabilized nematic phase where chemical constitution of the LCP matrix determines the $\langle S \rangle_r$ transition threshold. The guest and host stabilized nematic region corresponds to $w_{p,p} > w_{p,p}^c(\rho_r)$ and $w_{r,r} > w_{r,r}^c(\rho_r)$. Finally, $w_{r,r} > w_{r,r}^c(\rho_r)$ and $w_{p,p}$ crosses over the $w_{p,p} = w_{p,p}^c(\rho_r)$ line and triggers a spike like first order $N-N$ transition for the guest LC rods. This effect is also clearly seen in Fig. 2. The spike like $N-N$ transition takes place due to emergence of nematic ordering stabilized by the $N-I$ transition in the matrix with increasing matrix density. This is a first order $N-N$ transition. Below a special point the $N-N$ transition in LC rod ordering becomes the regular $N-I$ transition for the short rods.

The transition from guest–host to host stabilized orientational ordering does not have the hallmark of a phase transition, and a discontinuity in the order parameter was not observed. The continuity of $\langle S \rangle_r$ with ρ_r in the presence of the ordered LCP matrix at the critical $N-I$ transition density threshold of the LC rods in the absence of the matrix is apparent in Fig. 2. This strong LCP matrix effect on the phase diagram of the LC rods corresponds to the no transition line in Fig. 3. Phase regions in Fig. 3 are suggestive and are a projection of a 3D phase diagram onto a 2D plane. They must be understood in close proximity to the actual values of $w_{r,r}$ and $w_{p,p}$ in relation to the thresholds $w_{r,r}^c$ and $w_{p,p}^c$ as discussed earlier.

Figure 2 also depicts the effects of varying the guest–guest and host–host alignment interactions on orientational ordering. Decreasing $w_{p,p}$ shifts the $N-N$ host stabilized transition to lower LC rod densities (dashed thick line) yet the $N-N$ transition is more pronounced at lower $w_{p,p}$ and is most likely to be observed in experiments. At $w_{r,r}$ below 6.78 in the absence of matrix orientational ordering the LC rods are found always in the isotropic phase. Above the matrix $N-I$ transition a further decrease in matrix anisotropic interactions shifts the matrix stabilized LC rod $N-I$ transition to a lower density threshold (viz. dot dashed line). The effects of LCP backbone stiffness on orientational ordering of the LC rods are displayed in Fig. 4. A lower backbone stiffness increases the orientational entropy of the LC rods and disrupts their ordering. A lower LCP stiffness also shifts $N-N$ and the $N-I$ transitions to a lower rod density threshold. This effect is apparent from a comparison of the thick continuous line with the dashed line and the thin continuous line with the dot dashed line in Fig. 4.

Figure 5 displays the orientational phase diagram in density and temperature coordinates. The nematic phase is a union of regions located above the solid line and below the dashed line. The polymer conformations are frozen and there is no coexistence in the present case. Points c and d in small circles which bound the double headed horizontal line indicate one fixed critical density on the y axis. The high critical temperature at point d indicate a step host stabilized nematic isotropic transition. At point c a nematic–nematic transition from a host stabilized to a guest-host-stabilized state takes place. Note the equiordering point above at which the critical temperature for host and guest nematic ordering coincide.
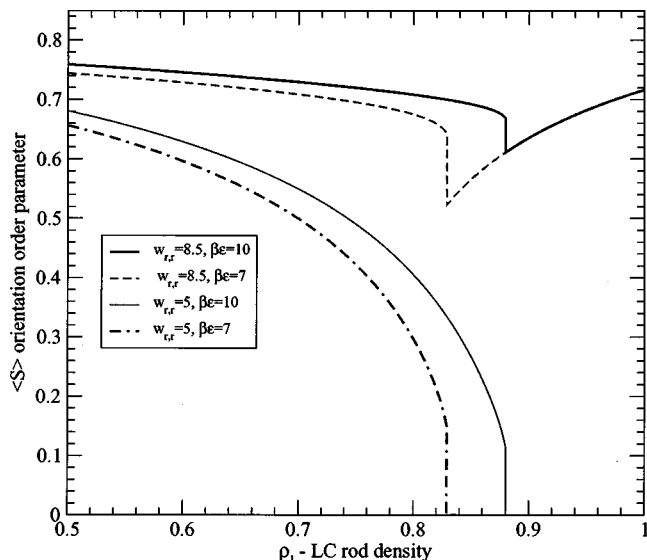
FIG. 4. Effect of variation of segment stiffness of LCP matrix on ordering of LC rods: $w_{p,r}=5$, $w_{p,p}=5$.

FIG. 6. Effect of varying softness temperatures on T, ρ phase diagram: $v_{p,p}=3$, $v_{r,r}=3$, and $\beta\epsilon=7$.

Above the equidistant ordering point phase inversion occurs and a high temperature guest stabilized nematic ordering occurs first. At a lower T the $N-N$ from a guest stabilized to a host stabilized region takes place.

The effects of varying the interaction softness of the rods and the polymer, i.e., T_r^s and T_p^s, are depicted in Fig. 6. The interaction softness has dramatic effect on the ordering threshold. An increase in the rod–rod softness shifts the guest stabilized threshold ρ_1^c to higher densities while the decrease in the polymer segment–polymer segment softness T_p^s shifts the host stabilized density threshold ρ_2^c to lower temperatures. Lowering T_p^s, the quenched matrix orders at higher N/I threshold density which sets a lower guest nematic ordering density threshold. This trait is apparent from comparison of the thick dashed and the thin dashed lines in Fig. 6.

The effect of varying the hard sphere interactions $v_{r,r}$ and $v_{p,p}$, displayed in Fig. 7, follows qualitatively the dependence on softness temperature displayed in Fig. 6 where only the scaling with critical temperature is different. Figure 8 depicts the effect of varying the guest–host interaction coupling on rod LC ordering. At high matrix densities the guest is bound to order essentially in anisotropic free volume cavities directed in a plane proportional to the matrix ordering. The guest–guest interaction may be high, as displayed by the thick dashed line of 8.5 kT in Fig. 8 and the increase in the cavity anisotropy has a stronger effect on ordering then decreasing the rod density. At low guest–host interaction alignment coupling, the decrease in rod density has a stronger effect and the LC rod ordering decreases with decreasing rod density. Another important effect related to the anisotropic coupling between the LCP chains and the LC rods is its effect on the magnitude of the discontinuity at the $N-N$ guest–host stabilized transition and host stabilized transition. (Compare the thick solid line with the thick dashed line and the thin solid line with the dotted dashed thick line at the
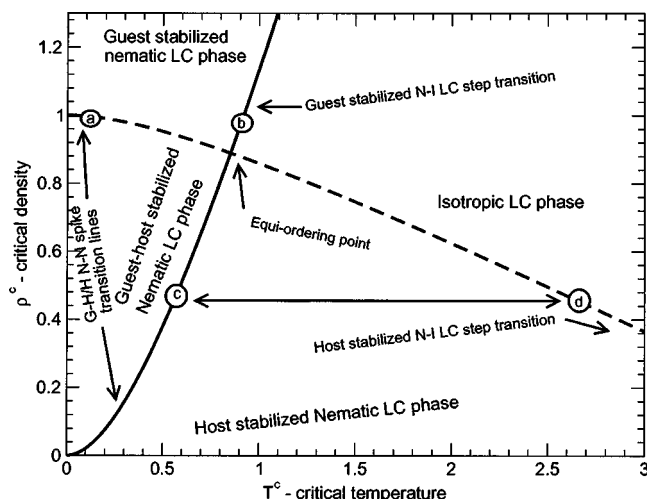

FIG. 5. Orientational phase diagram in temperature and density; guest and host softness temperatures are $T_r^s=1$ and $T_p^s=1$, respectively. Hard core alignment volume penalty for guest and host are $v_{p,p}=3$ and $v_{r,r}=3$, respectively. $\beta\epsilon=7$.
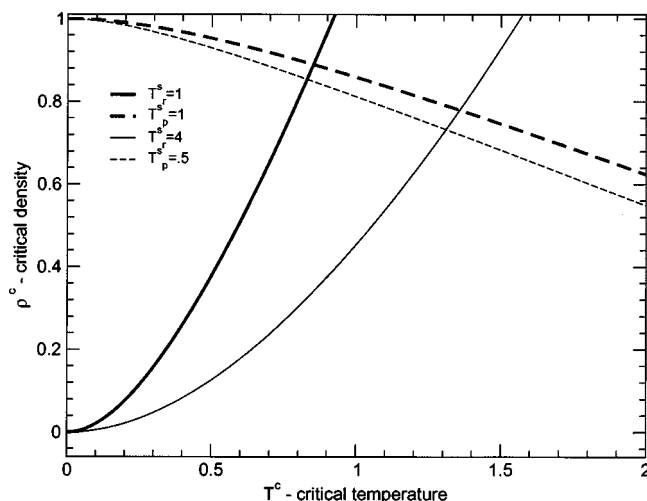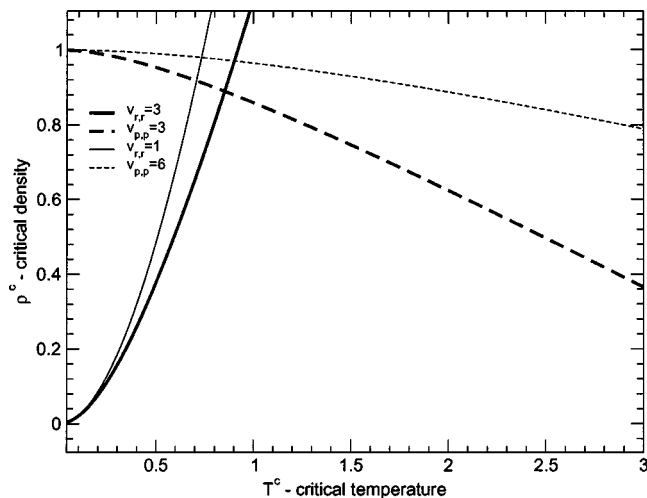

FIG. 7. Effect of varring the hard core alignment on orientational phase diagram: $T_r^s=4$, $T_p^s=0.5$, and $\beta\epsilon=7$.

J. Chem. Phys., Vol. 120, No. 23, 15 June 2004
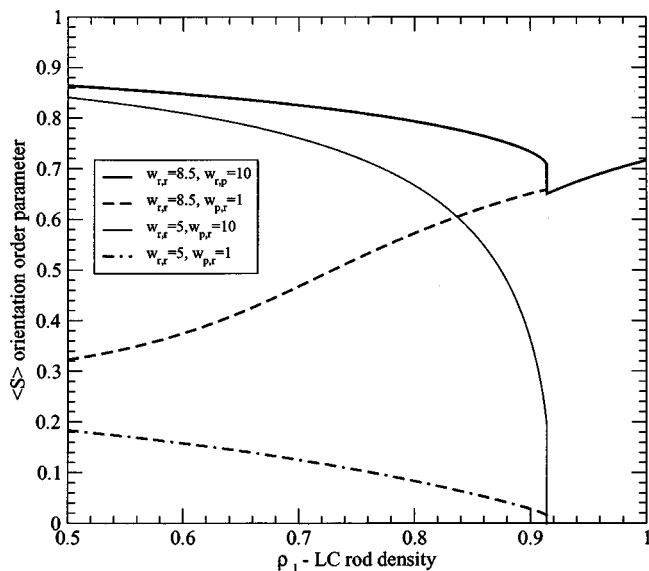
Phase and orientational ordering   11323

FIG. 8. Effect of varrying guest–host anisotropic interactions on ordering of LC rods: $w_{p,p}=10$, and $\beta\epsilon=7$.

transition). Variation of the guest–host anisotropic interactions in experiments is an ideal means for manipulating the magnitude of discontinuity of the orientational order parameter at the transition while retaining the transition density threshold value. This is true for both the $N-N$ and the $N-I$ transitions displayed in Fig. 8.

The discotic versus nematic ordering is displayed in Fig. 9. The discotic order parameter in the plane perpendicular to the polymer director is obtained by computing the LC nematic order parameter defined at $\theta=\frac{\Pi}{2}$ in Eq. (9). At low guest–host coupling the nematic ordering decreases with rod density as the LC rod discotic ordering is rather constant. At large guest–host couplings, i.e., $w_{p,r}=10$ the situation is different. The increase in LCP matrix density is progressively confining the LC rods in two dimensions and this effect is stronger then a linear decrease in rod density.
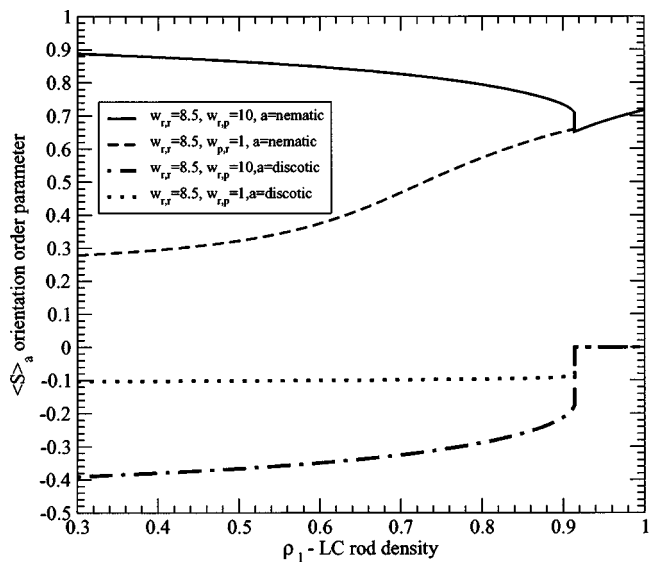

FIG. 9. Effect of varrying guest–host anisotropic interactions on nematic and discotic ordering of LC rods: $w_{p,p}=10$, and $\beta\epsilon=7$.
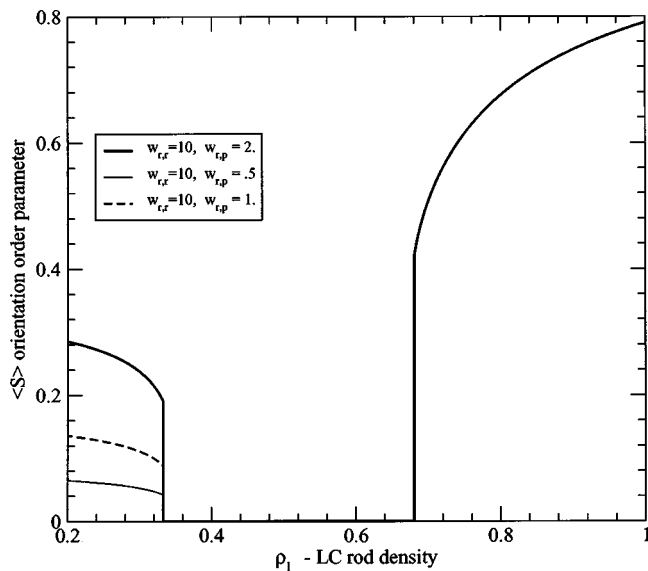

FIG. 10. The re-entrant orientational transition in guest–host LCP system: $w_{p,p}=10$, and $\beta\epsilon=7$.

Let us now consider the case of nonoverlapping phase boundaries. The orientational profile for this case is displayed in Fig. 10. A guest stabilized $N-I$ transition takes place with decreasing LC rod density. The high density $N-I$ transition threshold (thick line) is independent of the LCP matrix interaction anisotropy or guest–host interaction coupling as long as the LCP matrix is not ordered. At lower rod LC densities an $I-N$ re-entrant transition takes place. This re-entrant transition is induced by the emergence of orientational ordering in the LCP matrix. The LC director now points to the plane normal to the LCP director and is strongly effected by the guest–host interaction coupling. The effect of the LCP matrix LC rod interaction coupling is increasingly dominant as attested by $\partial\langle S\rangle_r/\partial\rho_r<0$ below the $I-N$ density threshold.

IV. RELEVANCE TO EXPERIMENTS AND COMPUTER SIMULATIONS

In this work we developed a statistical field theory for a guest–host system of low molecular weight LC rods in a LCP matrix with quenched backbone conformations and mobile side chains. Our predictions for the orientational phase diagram suggest new ways to optimize orientational properties of LC rods in a host polymer matrix. One prediction is the occurrence of a first order transition from a nematic phase stabilized by guest–guest interactions alone to a nematic phase stabilized by orientational ordering of the backbone LCP matrix. The dependence of the order parameter $\langle S\rangle_r$ on density in the vicinity of the host stabilized nematic–nematic transition has the appearance of a spike (Fig. 2) and is relevant to applications that require a simultaneous and discontinuous change in the guest director angle and orientational strength of $\langle S\rangle_r$. In a real liquid crystalline system $\langle S\rangle_r$ can be calculated from the dipolar splittings of NMR measurements.[2] Contributions from short range and long range interactions can be sorted out using NMR quadrupolar splittings of small probe solute molecules[38] immersed in the

liquid crystalline phase. In few nematic mixtures this method shows the presence of dominant short range interactions and negligible contributions from long range interactions (for example see Ref. 39). Other useful instrumental methods for analysis and characterization of orientational order are x-ray scattering, optical birefringence, and neutron scattering.[40]

Predictions from Hamiltonians with short range interactions are useful in studying orientational phase diagrams and also in understanding the physics displayed by complex liquid–crystalline systems. Hamiltonian based calculations were carried out for many chain polymer systems made of mesogens and flexible spacers with short range interactions,[41] and the phase diagrams predicted were found in qualitative agreement with experiments. In a separate study[42] using a more detailed field theoretic approach to derive the coupling among conformations and orientations, the typical nematic domain size was predicted in good agreement with the optical microscopy measurements by Stupp.[43]

Microscopic parameters of the Hamiltonian can be derived from the experiment or from a computer simulation. Assuming that a Landau–de Gennes expansion is valid the free energy parameters are readily expressed with microscopic interaction parameters of the Hamiltonian. The free energy parameters can be derived using experimental spectroscopic and calorimetric techniques,[44,45]

The systematic dependence of $\langle S \rangle_r$ and $\langle S \rangle_p$ on temperature and short rod density in the guest–host system studied here can be obtained using NMR measurements[38,40] without assuming a valid Landau–de Gennes expansion, i.e., a small value of orientation order parameter at the transition. Selective NMR deuteration can be used to measure $\langle S \rangle_r$ and $\langle S \rangle_p$ separately. The dependence of the Hamiltonian parameters $w_{r,r}$, $w_{p,p}$, and $w_{r,p}$ on temperature and density in our model can be obtained directly from best fit of the theoretical $\langle S \rangle_r$ and $\langle S \rangle_p$ to their derived values from NMR measurements. $\beta\epsilon$ can be obtained from separate small angle light scattering data of the polymer. This approach to derive the Hamiltonian coefficients from experiment is instrumental in exploring phase and orientational ordering in various regions of the phase diagram and rationalizing the experimental observations. Another instrumental method to determine orientational ordering in guest–host systems is from measurement of polarized UV–visible spectra of fluorescent dyes dissolved in the liquid crystalline host. This method has been applied successfully to a related guest–host system,[27] yet a systematic scan in density and temperature space has not been performed in the absence of a suitable theoretical model for analyzing the experiments.

In computer simulations of liquid crystalline systems, interaction potentials with various degrees of detail were proposed; they include: hard prolate/oblate ellipsoids, Guy Berne potentials,[50] and all atom potentials (see Ref. 38 for a short review). A reduced interaction representation in simulations can provide important insights into behavior of simplified models, the role of interaction nature, and liquid crystal aspect ratio on the orientational phase ordering (e.g., see Refs. 46–48). Predictions from all atom interaction models are more time consuming and the results depend strongly on a judicious choice of force fields. A conventional potential function with bond bending, torsional motion, and nonbonding interactions in a united atom representation molecular dynamics or Monte Carlo simulation is perhaps more useful. Molecular dynamics of 5CB in benzene with a united atom representation for the molecular interactions were carried out. The predictions from simulations were compared with 5CB orientational ordering and effective Mayer–Saupe (MS) interactions derived from NMR quadrupole splittings.[49] The MS interaction parameters for the mixture were computed and represented in terms of the average values of interaction pair potentials of the interacting species averaged over the intermolecular separations. These average interaction parameters and nematic orderings obtained in the simulation were found in good agreement with those derived from NMR experimental measurements; this study suggest another way coarse grained theories of liquid crystals can be useful.[49]

It could be interesting to carry out first a Monte Carlo simulation of the present model with the short range version of the Hamiltonian given in Eq. (1) and study the effect of the quenched polymer distribution on the magnitude of orientational ordering of the liquid crystalline rods, the shape of the order parameter dependence on short rod density in the vicinity of the the host stabilized nematic–nematic transition, and also to test the phase transition thresholds derived in the present work. We predict that varying the LCP chemical composition and/or thermodynamical variables in a manner that decreases the LCP backbone stiffness can partition this nematic–nematic transition in two nematic LC phases separated by an isotropic phase (see Fig. 10). This phase partitioning useful in applications that require optical switches sensitive to small density or/and temperature changes could be tested directly in a simulation of the model proposed herein. At a later stage, the interaction parameters in Eq. (1) can be derived from a united atom simulation and compared to those derived from experimental NMR couplings of a real guest–host system following the analysis steps proposed in Ref. 49.

ACKNOWLEDGMENTS

APPENDIX A: DERIVATION OF LC ROD ENTROPY

First we evaluate the entropy contribution from LC rods used to obtain the free energy in Eq. (9). The integration over centers of mass of the molecules yields the known Flory–Huggins for translational entropy. The LC orientational entropy is

$$S_{\text{LC orientation}} T/V = \int d\lambda_r \rho_r \log \int \prod_\alpha \frac{\exp(i\lambda_r)}{\sqrt{\psi_r^\alpha + i\lambda_r}}. \quad (A1)$$

J. Chem. Phys., Vol. 120, No. 23, 15 June 2004

Phase and orientational ordering 11325

Next we invoke cylindrical symmetry, i.e., the field σ_r and ψ_r components are either parallel or perpendicular to the director. With these symmetry considerations integrals over λ_r are performed. The result is

$$\frac{S_{LC}T}{V} = \rho_r \log(\rho_r) - \rho_r \log(2\pi^{1.5}) + \rho_r \psi_{l\perp}$$

$$- \rho_r \log\left(\pi^{1/2} \frac{\mathrm{erfi}\left(\sqrt{\psi_{l\perp} - \psi_{l\|}}\right)}{\sqrt{\psi_{l\perp} - \psi_{l\|}}}\right) - \psi_{l\perp}\sigma_{l\perp}$$

$$- 2\psi_{l\|}\sigma_{l\|}. \tag{A2}$$

APPENDIX B: DERIVATION OF LCP FREE ENERGY CONTRIBUTIONS

Let us now obtain the LCP contributions used in derivation of the free energy in Eq. (9). We now shift part of the propagator that involves integration over polymer coordinates from Lagrangian to Hamiltonian form.[35] This transformation allows us to do integrals over coupled polymer conformations and orientations for the LCP matrix. L is chain length and subscripts denote principal axis components. $\hat{\mathbf{p}}_\alpha$ and $\hat{\mathbf{u}}_\alpha$ are the α momentum and coordinate operators, ψ_α is the principal axis representation of the fields $\sqrt{-1}\psi^{jj}$, while λ_p equals $\sqrt{-1}$ times the auxiliary field that sets the magnitude of $\mathbf{u}(n_i)$ to 1 for the LCP segments in Eq. (5). The free energy is now computed in the limit of long LCP chains. Entropic orientational and conformational averages in the free energy are carried out using creation/annihilation operators (a^+, a) based on the Hamiltonian

$$H = \sum_\alpha \left(-\frac{1}{4A}\hat{\mathbf{p}}_\alpha^2 + h_\alpha \hat{\mathbf{u}}_\alpha^2\right)$$

with

$$\hat{\mathbf{u}}_\alpha = \frac{a_\alpha + a_\alpha^+}{\sqrt{2m\omega_\alpha}}, \quad \hat{\mathbf{p}}_\alpha = (a_\alpha - a_\alpha^+)\frac{\sqrt{m\omega_\alpha}}{2},$$

$$m = 2A, \quad \omega_\alpha = \left(\frac{h_\alpha}{A}\right)^{1/2},$$

and $[a_\alpha, a_\beta^+] = \delta_{\alpha,\beta}$.

Invoking global cylindrical symmetry, the total free energy per monomer in units of kT is

$$F = \frac{\rho_p}{2}\sqrt{\frac{\psi_{p,\|} + 2\psi_{p,\perp} + \lambda_p}{\dfrac{\beta\epsilon}{2}}} - \rho_p\lambda_p - (\psi_{p\|}\sigma_{p\|} + 2\psi_{p\perp}\sigma_{p\perp}) + \frac{w_{p,p}}{2}((\mathrm{Tr}\,\sigma_p)^2 - \mathrm{Tr}(\sigma_p:\sigma_p)) + w_{p,r}(\mathrm{Tr}\,\sigma_p\,\mathrm{Tr}\,\sigma_r$$

$$- \mathrm{Tr}(\sigma_p:\sigma_r)) + \frac{w_{r,r}}{2}((\mathrm{Tr}\,\sigma_r)^2 - \mathrm{Tr}(\sigma_r:\sigma_r)) + \rho_r\log(\rho_r) - \rho_r\log(2\pi^{1.5}) + \rho_r\psi_{l\perp} - \rho_r\log\left(\pi^{1/2}\frac{\mathrm{erfi}(\sqrt{\psi_{l\perp} - \psi_{l\|}})}{\sqrt{\psi_{l\perp} - \psi_{l\|}}}\right)$$

$$- \psi_{l\perp}\sigma_{l\perp} - 2\psi_{l\|}\sigma_{l\|}. \tag{B1}$$

The Flory–Huggins translational entropy contribution to LCP free energy is absent in Eq. (B1) since the backbone chain conformations are quenched. The first four terms in Eq. (B1) are nonlinear contributions to entropy from orientational and conformational averaging over the LCP chains, the fifth term is the constraint on unit length of the stiff mesogen, and the last terms are contributions from orientational tensors to energy.

APPENDIX C: DERIVATION OF GUEST–HOST COUPLING TERM

Next we calculate the guest–host coupling term $\mathrm{Tr}(\sigma_r:\sigma_p)$ and outline transformations required to derive the final form of these contributions to the free energy in Eq. (9). Most generally,

$$\mathrm{Tr}(\sigma_r:\sigma_p) = \mathrm{Tr}[T_\phi T_\phi^{-1}\sigma_r T_\phi T_\phi^{-1}T_\phi T_\phi^{-1}\sigma_p T_\phi T_\phi^{-1}], \tag{C1}$$

where T_ϕ is a transformation matrix from some arbitrary coordinate system to a new coordinate system in which σ_p is diagonal: $T_\phi^{-1}\sigma_p T_\phi = \sigma_p^{h,q}\delta_{h,q}$. Using this relation and the cyclic property of the trace yields

$$\mathrm{Tr}(\sigma_r:\sigma_p) = \sum_{l,h,q}\sigma_r^{l,h}\sigma_p^{h,q}\delta_{h,q}\delta_{l,q} = \sum_l \sigma_r^{l,l}\sigma_p^{l,l}. \tag{C2}$$

Next we invoke another set of order parameters used in the Landau–de Gennes expansion

$$\bar{Q}_r = \langle S\rangle_r (3\underline{n}\,\underline{n} - \underline{I});$$

$$\bar{Q}_p = \langle S\rangle_p (3\underline{n}\,\underline{n} - \underline{I}). \tag{C3}$$

The projection of Q onto a space $|p\rangle|q\rangle$ is defined as: $Q_r|r\rangle|q\rangle = \langle S\rangle_r (3n_l n_q - \delta_{l,q}); \quad Q_p|r\rangle|q\rangle = \langle S\rangle_p (3m_l m_q - \delta_{l,q})$. The relation between Q and the orientational tensor σ allows us to obtain a general relation among projection of directors of different species, the orientation order parameters, and the orientational tensor matrix

$$\sigma_r^{l,q} = \frac{\rho_r}{3}(\delta_{l,q} + \langle S\rangle_r (3n_q n_l - \delta_{l,q}));$$

$$\sigma_p^{h,q} = \frac{\rho_p}{3}(\delta_{h,q} + \langle S\rangle_p (3m_h m_q - \delta_{h,q})). \tag{C4}$$

Let us now consider the principal axis representation of $\sigma_\perp^p$, $\sigma_\|^p$ and $\sigma_\perp^p$, $\sigma_\|^p$:

$$\sigma_\perp^p = \frac{\rho_p}{3}(1+2\langle S\rangle_p);$$

$$\sigma_\parallel^p = \frac{\rho_p}{3}(1-\langle S\rangle_p); \tag{C5}$$

and

$$\sigma_\perp^r = \frac{\rho_r}{3}(1-\langle S\rangle_r);$$

$$\sigma_\parallel^r = \frac{\rho_r}{3}(1+2\langle S\rangle_r). \tag{C6}$$

The director of $\sigma_\perp^p$ is chosen in Eqs. (C5) and (C6) parallel to the $\sigma_\parallel^r$ director. The relation of $\mathbf{n}_\parallel$ to $\mathbf{m}_\parallel$ defines the principal axis. The choice of principal axis employed in Eqs. (C5)–(C6) implies that $\langle S\rangle_r$ is probed at a $\pi/2$ angle in relation to $\langle S\rangle_p$. A positive value for $\langle S\rangle_r$ describes rod ordering in the plane perpendicular to the polymer matrix director.

APPENDIX D: DERIVATION OF EQ. (9)

Let us now discuss derivation of the free energy in Eq. (9) expressed with $\langle S\rangle_r$ and $\langle S\rangle_p$. Using saddle points we obtain the free energy dependence on orientational tensor σ_p and the Lagrange multiplier λ_p for the LCP matrix. This calculation does not involve coupling of LCP to the LC rods. The LCP backbone conformations are quenched and equilibration of the LCP backbone conformations to the LC rods is not possible. The LCP orientational fields obtained from this SCF calculation are used later on as input and act as external fields in the numerical calculation of orientational LC ordering. The SCF LCP calculation yields $\psi_p's(\sigma_p's)$. ψ_p fields are now eliminated from free energy in favor of σ_p's. Next we use the relations among σ_p and $\langle S\rangle_p$ and σ_r and $\langle S\rangle_r$ discussed in context of Eq. (7), and the free energy is now expressed with $\langle S\rangle_p$ and $\langle S\rangle_r$ and λ_p in Eq. (9).

[1] L. Gutman, J. Cao, T. M. Swager, and E. L. Thomas, Chem. Phys. Lett. **389**, 198 (2004).
[2] P. G. de Gennes, *The Physics of Liquid Crystals* (Clarendon, Oxford University Press, Oxford, 1974).
[3] R. Moldovan, Cryst. Res. Technol. **35**, 1315 (2000).
[4] W. Mayer and A. Z. Saupe, Naturforscher **12**, 882 (1959).
[5] P. J. Collings and M. Hird, *Introduction to Liquid Crystals, Chemistry and Physics* (Taylor and Francis, London 1997).
[6] I. W. Hamley, S. Garnett, S. R. Luckhurst, and S. J. Roskilly, J. Chem. Phys. **104**, 10046 (1996).
[7] S. D. Gottke, D. D. Brace, H. Cang, and M. D. Fayer, J. Chem. Phys. **116**, 360 (2002).
[8] H. Cang, J. Li, V. N. Novikov, and M. D. Fayer, J. Chem. Phys. **119**, 10421 (2003).
[9] A. M. Mayes and M. Olivera de la Cruz, Acta Metall. **37**, 615 (1989).
[10] J. Ilnytskyi and S. Sokolowski, Phys. Rev. E **59**, 4161 (1999).
[11] H. Zheng, B. Zalar, G. S. Iannacchione, and D. Finotello, Phys. Rev. E **60**, 5607 (1999).
[12] A. Matsuyama and T. Kato, J. Chem. Phys. **108**, 2067 (1998).
[13] F. BenMouna, A. Daoudi, F. Roussel, J. M. Bousine, X. Coqueret, and U. Maschke, J. Polym. Sci., Part B: Polym. Phys. **37**, 1841 (1999).
[14] A. Mertelj, L. Spindler, and M. Copic, Phys. Rev. E **56**, 549 (1997).
[15] E. Berggren and C. Zannoni, Phys. Rev. E **49**, 614 (1994).
[16] F. Roussel, C. Canlet, and B. M. Fung, Phys. Rev. E **65**, 021701 (2002).
[17] Y. V. Pereverzev, O. V. Prezhdo, and L. R. Dalton, Chem. Phys. Lett. **340**, 328 (2001).
[18] Y. V. Pereverzev, O. V. Prezhdo, and L. R. Dalton, J. Chem. Phys. **117**, 3354 (2002).
[19] A. W. Harper, S. Sun, L. R. Dalton, S. M. Garner, A. Chen, S. Kalluri, W. H. Steierand, and B. H. Robinson, J. Opt. Soc. Am. B **15**, 329 (1999).
[20] B. H. Robinson, L. P. Dalton, A. W. Harper *et al.*, Chem. Phys. **245**, 35 (1999).
[21] A. K. Y. Jen, Y. W. Liu, L. X. Zheng, S. Liu, K. Y. Drost, Y. Zhang, and L. R. Dalton, Adv. Mater. (Weinheim, Ger.) **11**, 452 (1999).
[22] M. I. Boamfa, K. Viertler, A. Wewerka, F. Stelzer, P. C. M. Christiansen, and J. C. Maan, Phys. Rev. E **67**, 050701 (2003).
[23] D. Stewart and C. T. Imrie, Macromolecules **30**, 877 (1997).
[24] T. Kato, N. Hirota, A. Fujishima, and J. M. Frechet, J. Polym. Sci. A **34**, 57 (1996).
[25] H. W. Chiu, Z. L. Zhou, T. Kyu, L. G. Cada, and L. C. Chien, Macromolecules **29**, 1051 (1996).
[26] M. C. Chang, H. W. Chiu, X. Y. Wang, T. Kyu, N. Leroux, S. Campbell, and L. C. Chien, Liq. Cryst. **25**, 733 (1998).
[27] T. M. Long and T. M. Swager, J. Am. Chem. Soc. **124**, 3826 (2002).
[28] Z. Zhu and T. M. Swager, J. Am. Chem. Soc. **124**, 3826 (2002).
[29] T. M. Long and T. M. Swager, J. Mater. Chem. **12**, 3407 (2002).
[30] G. H. Fredrickson and L. Leibler, Macromolecules **23**, 531 (1990).
[31] A. M. Gupta and S. F. Edwards, J. Chem. Phys. **98**, 1588 (1993).
[32] R. Holyst and P. Oswald, Macromol. Theory Simul. **10**, 1 (2001).
[33] R. Holyst and M. Schick, J. Chem. Phys. **96**, 721 (1992).
[34] R. Holyst and M. Schick, J. Chem. Phys. **96**, 730 (1992).
[35] M. Swanson, *Path Integrals and Quantum Processes* (Academic, Harcourt Brace Jovanovich, New York, 1992).
[36] S. Wolfram, *The Mathematica Book*, 4th ed. (Cambridge University Press, Cambridge, 1999).
[37] A. Tkachenko and Y. Rabin, Macromolecules **28**, 8646 (1995).
[38] E. E. Burnell and C. A. de Lange, Chem. Rev. (Washington, D.C.) **98**, 2359 (1998).
[39] R. T. Syvitski and E. E. Burnell, Chem. Phys. Lett. **281**, 199 (1997).
[40] *Phase Transitions in Liquids Crystals*, edited by S. Martellucci and A. N. Chester, NATO ASI Series, Series B: Physics (Plenum, New York, 1992), Vol. 290.
[41] X. J. Wang and M. Warner, in *Phase Transitions in Liquids Crystals*, edited by S. Martellucci and A. N. Chester, NATO ASI Series, Series B: Physics (Plenum, New York, 1992), Vol. 290, Chap. 25.
[42] L. Gutman, E. I. Shakhnovich, Chem. Phys. Lett. **325**, 323 (2000).
[43] P. G. Martin and S. I. Stupp, Macromolecules **21**, 1222 (1988); **21**, 1288 (1988).
[44] J. Thoen, in *Phase Transitions in Liquids Crystals*, edited by S. Martellucci and A. N. Chester, NATO ASI Series, Series B: Physics (Plenum, New York, 1992), Vol. 290, Chap. 10.
[45] C. W. Garland, in *Phase Transitions in Liquids Crystals*, edited by S. Martellucci and A. N. Chester, NATO ASI Series, Series B: Physics (Plenum, New York, 1992), Vol. 290, Chap. 11.
[46] D. Frenkel, Mol. Phys. **55**, 1171 (1985).
[47] D. Frenkel, Mol. Phys. **60**, 1 (1987).
[48] D. Frenkel, B. Muler, and J. P. McTague, Phys. Rev. Lett. **52**, 287 (1984).
[49] D. Sandstrom, A. V. Komolkin, and A. Maliniak, J. Chem. Phys. **104**, 9620 (1996).
[50] A. V. Lyulin, M. S. Al-Barwani, M. P. Allen, M. R. Wilson, I. Neelov, and N. K. Allsopp, Macromolecules **31**, 4626 (1998).